DOI: 10.1002/cmdc.200800020

Conformationally Restricted Hydantoin-Based Peptidomimetics as Inhibitors of Caspase-3 with Basic Groups Allowed at the S_3 Enzyme Subsite

Jesús Vázquez,[b] Alicia García-Jareño,[a] Laura Mondragón,[a] Jaime Rubio-Martinez,[c] Enrique Pérez-Payá,*[a] and Fernando Albericio*[b, d, e]

By using a combination of molecular modeling, combinatorial chemistry, and biological essays, novel scaffold molecules for the inhibition of caspase-3 have been developed. These compounds have an overall attenuated negative charge and show similar IC_{50} values for both recombinant and human endogenous caspase-3. This might provide the basis for a novel strategy for the discovery of potent and more druglike inhibitors of caspase-3.

Introduction

Apoptosis, or programmed cell death, which was first described in 1972,[1] plays a key role in the maintenance of homeostasis in multicellular organisms. Defects in the regulation of apoptosis could be at the molecular basis of several diseases. This biochemical process is complex and sophisticated, and involves a large number of proteins that are located mainly in the cell membrane, cytoplasm, mitochondrion, and nucleus.[2] Apoptosis is regulated by a family of proteases called caspases, which are highly homologous and regulated cysteine proteases that cleave specific aspartate-containing substrates.[3] At least 14 mammalian caspases are known to date, including 11 human caspases, which show several similarities in their structure, residue sequence, and substrate specificity.[4] Caspases are commonly divided into two groups depending on their function: inflammatory (e.g. caspases 1, 4, 5, and 13) or apoptotic. The latter can be further subdivided into effectors (e.g. caspases 3, 6, and 7), which are responsible for the disassembly of cellular components, and initiators (e.g. caspases 8, 9, and 10), which activate the effector caspases. A key mediator of apoptosis is caspase-3 because it is activated in nearly every model of this process. This enzyme is therefore an attractive target to explore the role of caspase inhibition for future applications in the treatment of diseases such as myocardial infarction, stroke, sepsis, traumatic brain injury, Parkinson's disease, or Alzheimer's disease, in which inappropriate apoptosis could be of relevance.[5–9] The active sites of all caspases have two main groups of residues, the catalytic diad, which includes a Cys and a His residue, and the group that comprises two Arg residues and one Gln, which is responsible for the aspartate specificity of caspases.[10] In fact, to engage the catalytic Cys residue, the active sites of all caspases require an aspartyl functionality in the P_1 amino acid position and an electrophilic carbonyl.[11] Peptidomimetic inhibitors of caspases have been reported[12–15] and all incorporate aspartyl functionality plus an electrophilic center (or warhead) for covalent attachment to the active site. While these chemical features are needed for high-affinity binding, they are not appropriate for cellular assays. Thus, the activity of most caspase-3 inhibitors is greatly attenuated, and even in the presence of cell extracts the decrease in potency is, in most cases, up to two orders of magnitude less than isolated caspase-3.[16] Thus, more selective, stable, and cell-permeable caspase-3 inhibitors are required. An ongoing program in our laboratories is focused on the design and identification of new building blocks that induce conformational restriction in the backbone of future druglike caspase-3 inhibitors. We initially focused on the hydantoin ring (Figure 1 a), which applies a local conformational restriction by the formation of a five-member ring angle that binds two consecutive N atoms of a peptide with a carbonyl moiety. Initial studies using a series of hydantoin-restricted peptides with an Asp residue in P_1 revealed that the ring could be accommodated in the active site of caspase-3.[17] Herein we report the optimization of this new family of caspase-3 inhibitors. These compounds tolerated the presence of basic residues that occupy the S_3 subsite of the

[a] *A. García-Jareño, L. Mondragón, Prof. E. Pérez-Payá*
Medicinal Chemistry Department
Centro de Investigación Príncipe Felipe and
Instituto de Biomedicina de Valencia, CSIC
Avda. Autopista del Sales 16, 46013 Valencia (Spain)
Fax: (+34) 963-289-680
E-mail: eperez@cipf.es

[b] *Dr. J. Vázquez, Prof. F. Albericio*
Institute for Research in Biomedicine
Barcelona Science Park, Josep Samitier 1, 08028 Barcelona (Spain)
Fax: (+34) 93-403-7126
E-mail: albericio@irbbarcelona.org

[c] *Prof. J. Rubio-Martinez*
Department of Physical Chemistry, University of Barcelona
Martí i Franqués 1, 08028 Barcelona (Spain)

[d] *Prof. F. Albericio*
Department of Organic Chemistry, University of Barcelona
Martí i Franqués 1, 08028 Barcelona (Spain)

[e] *Prof. F. Albericio*
CIBER-BBN
Networking Centre on Bioengineering, Biomaterials and Nanomedicine
Barcelona Science Park, Josep Samitier 1, 08028 Barcelona (Spain)

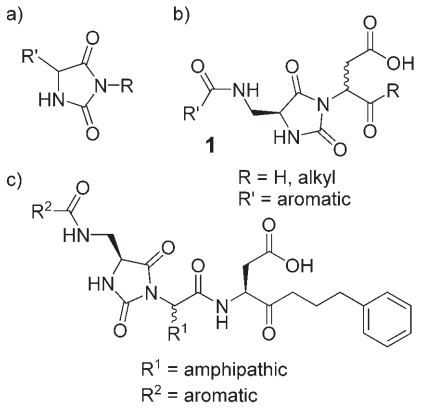

Figure 1. a) General structures of a) the disubstituted hydantoin ring, b) the compounds initially analyzed, and c) compounds with distinct amphipathic residues.

enzyme, thereby decreasing the overall negative charge of the inhibitors.

Results and Discussion

Preliminary work performed by our research group showed that the hydantoin ring **1** (Figure 1 b) fits into the caspase-3 active site, and therefore compounds that were based on the general structure of **1** were synthesized.[17] The initial assays for caspase-3 inhibition revealed promising results. However, in silico analysis by molecular dynamics of these compounds suggested that the first step towards optimization should focus on the insertion of an additional spacer residue between the aspartyl and hydantoin moieties (Figure 1 c). After the synthesis of several compounds that had amphipathic residues with distinct side chain volumes, the best inhibitory results were obtained when aminoisobutyric acid (Aib) was used as a spacer.[17]

The potency and selectivity of caspase inhibitors depends on the structure of the backbone, exposed side chains, and the chemical reactivity of the warhead. We thus synthesized a first generation of compounds (Figure 2), by focusing on the side chain functionalities to be incorporated in the hydantoin ring and on the presence of aldehyde or phenylpropyl ketones at the carbonyl group of the P_1 aspartic acid residue (Figure 2).

A total of 18 compounds in an epimeric mixture at Cα of the aminobutyric acid residue were obtained. After evaluation of the inhibitory activity of these compounds, three (**13**, **14**, and **15**) showed IC_{50} values and enough chemical novelty to deserve further attempts at optimization (Table 1).

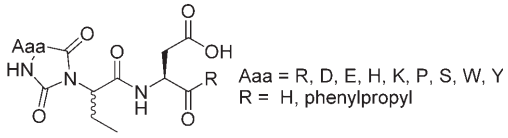

Figure 2. General structure of the first generation of compounds.

Table 1. Caspase-3 inhibition by P_3 residue substitution on hydantoin P_1 aldehydes.

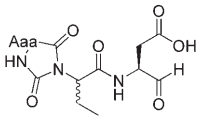

Compd	Residue (Aaa)	IC_{50} [μM]
13	Asp	81
14	Glu	32
15	Arg–Pbf[a]	41

[a] Pbf = 2,2,4,6,7-pentamethyl-2,3-dihydro-1-benzofuran-5-sulfonyl; structure shown in Figure 4 and Table 2.

Compounds **13** and **14**, which have the canonical acidic residue that is exposed to the S_3 subsite of caspase-3 match the systematic studies that have been reported in the literature on the specificity towards substrate peptides at this site (Figure 3).[10,11] In fact, molecular dynamic studies demonstrated

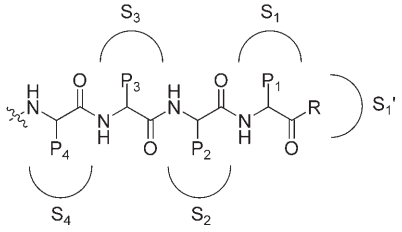

Figure 3. Standard nomenclature for the interaction between a tetrapeptide (P_4–P_1) with the various substrate binding sites (S_4–S_1').

that all three compounds fitted in the active site of caspase-3, thereby achieving a robust disposition inside (not shown). Furthermore, the hydrogen bond network of **15** was similar to that obtained for **13**, and additional hydrophobic interactions of the Pbf group with aromatic residues in the periphery of the caspase-3 active site were suggested by the output of the analysis (Figure 4).

Compound **15**, with its Pbf-protected guanidine group in which most of the reported caspase inhibitors have an acidic residue, raised our interest and was further selected for optimization. The single synthesis of the L isomer **15a**, instead of the epimeric mixture, increased the inhibitory activity by one order of magnitude (IC_{50} = 3.9 μM). Next, we examined distinct substitutions of the guanidine group in the Arg side chain. Analogues of **15a** with electron-withdrawing groups such as aromatic sulfonyl groups (in **16**–**18**), or nitrated **19**, as well as compounds with tetraalkylated guanidines **20**–**24** were synthesized. Electron-deficient guanidine compounds **16**–**19**, including the one that was only nitrated (compound **19**), showed similar activity to that of **15a** (Table 2).

Tetraalkylated compounds **20**–**24** were synthesized from the primary amine of the ornithine (Orn) side chain under mild conditions with aminium salts, by following previously de-

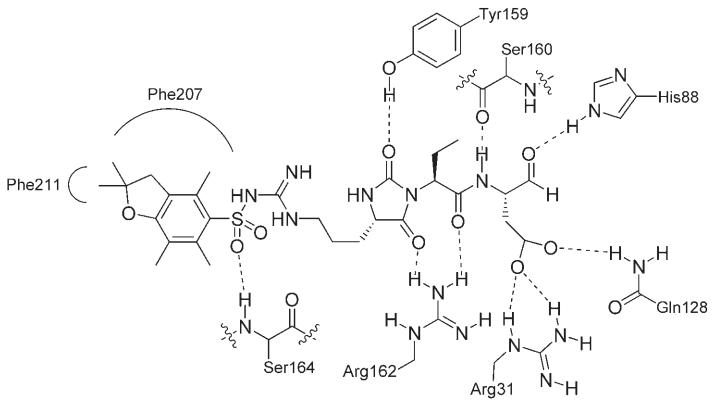

Figure 4. Interactions between the L isomer of **15** with caspase-3 found by molecular dynamics; numbers describe the order of the residues in PDB entry 1PAU.

scribed methodology that was developed by our group (Figure 4).[18] However, compounds **20**–**24**, together with the control compound **25**, showed a decrease in inhibitory activity. These results indicated that it is crucial to have a surrogate that is bonded to the guanidine function that has the capacity to form hydrogen-bonding interactions, for instance SO_2 or NO_2, that can interact with the basic residue at the S_3 subsite. It should be noted that the linear analogue of **15a** showed a significant decrease in activity (compound **26**, Table 2), thereby reinforcing the importance of the conformational restriction that is imposed by the hydantoin ring in these new caspase-3 inhibitors.

A series of compounds, **15a**, **17**, **19** and **27** were selected for further investigation by using extracts and whole cellular systems. Thus, we tested whether these compounds had the capacity to inhibit cellular caspase-3 in the same way that they inhibited recombinant caspase-3. We used a cell-free system that was obtained from HEK 293 cells.[19] When this extract was incubated at 37 °C in the presence of dATP, the caspase activity was activated, and could be followed by means of fluorogenic caspase-3 substrates.[20] The extent of caspase-3 activity was remarkably diminished, and importantly, the IC_{50} values that were obtained in this ex vivo system were remarkably similar to those that were obtained in the in vitro assay (Table 2). Furthermore, initial examination of the viability of these compounds in whole-cell-based models of apoptosis suggested low unspecific cell toxicity (as determined by MTT assays— see the Experimental Section for details) together with a modest capacity to inhibit apoptosis. To study whether these molecules inhibited programmed cell death, assays with U937 human histiocytic lymphoma cells that had been challenged with doxorubicin were performed in culture. In this cell-based model, doxorubicin induces apoptosis through DNA damage-activating executioner caspases. In addition, we also evaluated a more well-defined model of "only intrinsic" apoptosis by using Saos-2 cells, in which programmed cell death is induced by the doxycycline-dependent conditional expression of Bax through the tet-ON system (Clontech). Bax is a proapoptotic member of the Bcl-2 family that induces apoptosis by the release of cytochrome *c* from the mitochondria,[21] thus the activation of apoptosis relies solely on the mitochondrial pathway. When cells were treated with the apoptotic insult (doxorubicin or doxycycline for U937 or Saos2, respectively) in the presence of **15a**, **17**, **19** and **27** at 100 μM, the extent of apoptosis was diminished (except for **19**) as determined by the percentage of cell recovery. Moreover, the cell recovery values increased when cells were pretreated with the caspase-3 inhibitors before the addition of the apoptotic insult (Table 3).

In particular, **15a** showed considerable activity in the cellular assays. Given its chemical novelty, we think that this compound could serve as a lead for the generation of future, more druglike inhibitors of caspase-3. In a first approach for improvements, we aimed to decrease the chemical reactivity of the warhead. In early in vitro assays, the aldehyde-based analogues were more active than those based on aminomethyl ketone. However, the chiral instability and unspecific reactivity of α-amino aldehydes compromise their in-cell activity and compound selectivity.[22] These observations highlight the importance of alternative substitutes in caspase-3 peptide-based inhibitors at the P_1' position. We therefore synthesized a new family of compounds to analyze distinct substitutions in the P_1' site of **15a**. The first step of the synthesis was the incorporation of the α-chloromethyl ketone **8** to a semicarbazide resin, which was then treated with several nucleophiles like thiols, alcohols and secondary amines (Table 4).

The hydantoin ring was formed with a Pbf-protected Arg[23] for all of these nucleophiles, and very good yields were achieved for the thiols. In contrast, the alcohols and the secondary amines did not give such good results, probably because the former are not good nucleophiles and the latter are too basic. The new set of compounds was assayed for inhibitory activity and several features of interest were observed. Thus, compound **30**, which has an *S*-methylphenyl chain, showed biological activity (in vitro, in cell extracts, and in whole-cell assays) similar to that of **15a**. Furthermore, a comparison between compounds **29**, **31** and **34**, which differ only in the nature of the heteroatom at ε-position with respect to the ketone indicated that heteroatom selectivity might be involved in the interaction at the active site of caspase-3. This will be examined in future studies.

Conclusions

We have developed a novel set of scaffold molecules for the inhibition of caspase-3. These compounds have an overall attenuated negative charge and show similar IC_{50} values for both recombinant and human endogenous caspase-3. This might provide the basis for a novel strategy for the discovery of potent and more druglike inhibitors of caspase-3. Although results indicate that there is some loss of activity when comparing values that were obtained in ex vivo (i.e., cell extracts) with whole-cell experiments, we are proceeding with the next level of complexity, which is an appropriate in vivo model. If the compounds analyzed herein further demonstrate a capacity to

Table 2. Inhibition of caspase-3 activity.

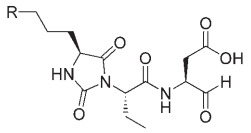

Compd[a]	R	Activity assays[b] In vitro IC_{50} [μM]	Cell extract IC_{50} [μM][c]
15a	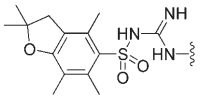	3.9 ± 0.7	4.5
16	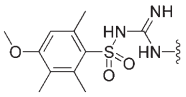	4.8 ± 0.3	ND
17	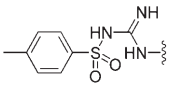	4.6 ± 0.8	2.5
18	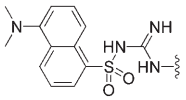	3.6 ± 0.6	ND
19	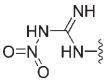	5.9 ± 1.2	5.3
20	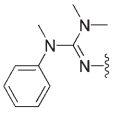	365	ND
21	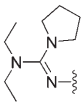	81	ND
22	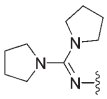	41	ND
23	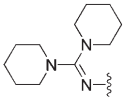	79	ND
24		29	ND
25		65	ND
26[d]	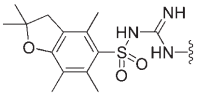	19	ND
27	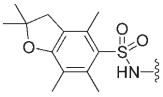	3.7	5.2

[a] L isomers. [b] See Experimental Section for details. [c] ND = not determined. [d] Linear compound as *N*-acetyl, without hydantoin ring formation.

decrease apoptosis in vivo, the optimization of their structures to increase their overall potency would be a motivating challenge.

Table 3. Evaluation of compound-dependent cell recovery after apoptotic insult.

Compd	Cell recovery [%][a] U937	Saos-2[b]
None	0	0
15a	46 ± 5	22 ± 3
17	25 ± 4	ND
19	0	ND
27	25 ± 8	14 ± 6

[a] After apoptotic insult in cells pretreated with the compounds; data expressed as mean ± SE ($n > 3$); see Experimental Section for details. [b] ND = not determined.

Table 4. Caspase-3 inhibition by P_1' substitution on Pbf-protected arginine hydantoins.

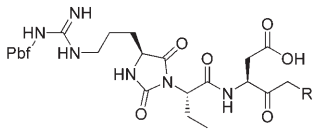

Compd	R	IC_{50} [μM][a]
29	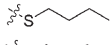	20
30	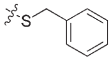	3.4
31	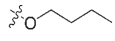	74
32	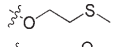	22
33	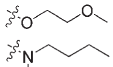	ND
34	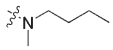	8.7
35		6.9

[a] ND = not determined.

Experimental Section

Chemistry

Methods. Solid-phase syntheses were carried out in polypropylene syringes that were fitted with polyethylene filter disks. Coupling reagents, solvents for peptide synthesis and other reagents were purchased from commercial suppliers at the highest purity available and were used without further purification. Analytical HPLC was performed by using a Waters Alliance 2695 (Waters, MA, USA) chromatography system with a PDA 995 detector, a reversed-phase Symmetry C_{18} column (4.6 × 150 mm, 5 μm) column and linear gradients of MeCN with 0.036% trifluoroacetic acid (TFA) into H_2O with 0.045% TFA. The system was run at a flow rate of 1.0 mL min^{-1} over 15 min. Semipreparative HPLC was carried out on a Waters chromatography system with a dual absorbance detector 2487, a reversed-phase Symmetry C_{18} column (30 × 150 mm, 5 μm) column and linear gradients of MeCN with 0.05% TFA into H_2O with 0.1% TFA. The system was run at a flow rate of 20.0 mL min^{-1} over 30 min. HPLC–MS was performed using a Waters Alliance 2796 with a dual absorbance detector 2487 and ESI-MS Micromass ZQ (Waters) chromatography system, a reversed-phase Symmetry 300 C_{18} (3.9 × 150 mm, 5 μm column) and H_2O

with 0.1% formic acid and MeCN with 0.07% formic acid as mobile phases. Mass spectra were recorded on a MALDI Voyager DE RP time-of-flight (TOF) spectrometer (Applied Biosystems, Foster City, CA, USA) by using ACH matrix.

Synthesis of Fmoc-protected aspartyl aldehydes and ketones. All the aspartyl derivatives were prepared from commercial *N*-Fmoc-Asp(O*t*Bu)-OH (**2**). Phenylpropyl ketone **4** was synthesized in two steps through 2-thiopyridine thioester by following a method that was developed previously in our laboratory.[24] The 2-thiopyridine thioester was reacted with the organocopper reagent to obtain the corresponding ketone in good yield (Scheme 1). The synthesis of aspartyl aldehyde **6** was performed by a reduction of the activated carboxylic acid to alcohol with $NaBH_4$ and then by an oxidation under Swern conditions (Scheme 1). Finally the α-chloromethyl ketone **8** was prepared through the diazoketone derivative, which, after treatment of aqueous HCl, afforded the final product in good yield (Scheme 1).[18]

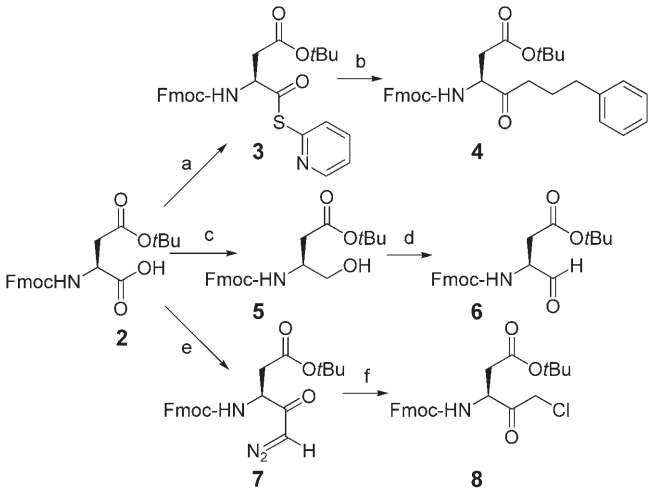

Scheme 1. Synthesis of Fmoc-protected aspartic acid derivatives. Reagents and conditions: a) 1-ethyl-3-[3-(dimethylamino)propyl]carbodiimide (1 equiv), 2-thiopyridine (1.1 equiv), CH_2Cl_2 (anhyd), room temperature; b) $Ph(CH_2)_3CuMgI$ (3 equiv), THF (anhyd), −78→0 °C; c) isobutylchloroformate (1.1 equiv), *N*-methylmorpholine (1.1 equiv), THF (anhyd), −78 °C, then $NaBH_4$ (2 equiv); d) Dess–Martin periodinane (1 equiv), CH_2Cl_2 (anhyd), room temperature; e) isobutylchloroformate (1.1 equiv), *N*-methylmorpholine (1.1 equiv), THF (anhyd), 0 °C then diazomethane (1.5 equiv), −50 °C; f) HCl (1 equiv), THF (anhyd), 0 °C.

Library solid-phase synthesis. Preparation of the libraries was carried out in the solid-phase by attaching either the Asp-based aldehyde or the ketone through the carbonyl group to a semicarbazide resin **9**, which was previously chosen as the most convenient after screening four hydrazine-based resins.[25] Resin **9** was synthesized from an aminomethyl by treatment with 1,1′-carbonyldiimidazole (CDI) in *N*,*N*-dimethylformamide (DMF) to activate the amine, followed by reaction with *tert*-butylcarbazate; this provided nearly quantitative loading levels. Initially, the Boc group was removed with a mixture of TFA/CH_2Cl_2 (1:1) followed by neutralization with DIEA/CH_2Cl_2 (1:19). The incorporation of the Fmoc-Asp(O*t*Bu)-$(CH_2)_3$-phenyl was performed by treating **9** with a CH_2Cl_2 solution of the ketone for 16 h at room temperature. Removal of the Fmoc group with piperidine/DMF (1:4) and further analysis by UV_{301} (7800 $M^{-1}cm^{-1}$) of its piperidine adduct showed that the incorporation the first building block had taken place quantitatively (Scheme 2).

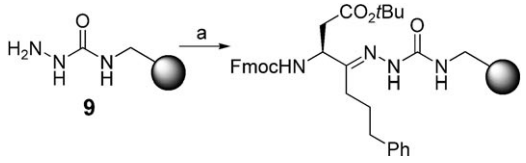

Scheme 2. Hydrazine-based polymer used and first residue incorporation. Reagents and conditions: a) Fmoc-Asp(O*t*Bu)-$(CH_2)_3$-Ph, CH_2Cl_2 (anhyd), room temperature.

Hydantoin synthesis. Our research group has reported two efficient methods for the solid-phase synthesis of hydantoin-peptides.[26,27] First, a method that involves epimerization of the α-carbon of the first amino acid and the second, which overcomes this side reaction.[27] First of all, the method that involved the epimerization of the Cα center of the residue immediately before was followed with the idea to explore a greater diversity (mixture of epimers). This method uses *N*,*N*-disuccinimidyl carbonate (DSC) as carbonylating reagent in the presence of a catalytic amount of 4-dimethylaminopyridine (DMAP) and basic treatments with K_2CO_3 in a solution of 0.4 M 18-crown-6 in DMF. The second method, which avoided epimerization featured the use of CDI as a carbonylating reagent, and a solution of DIEA/DMF (1:4) for the basic treatments (Scheme 3).

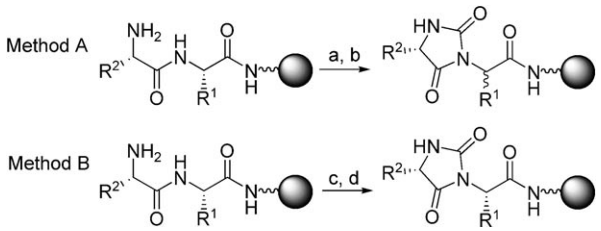

Scheme 3. General synthesis of hydantoins. Reagents and conditions: a) DSC (10 equiv), DMAP (1 equiv), room temperature; b) K_2CO_3 (5 equiv), 18-crown-6 (0.4 M), DMF, room temperature; c) CDI (5 equiv), DMF, room temperature; d) DIEA/DMF (1:4).

Guanidine formation. Tetraalkylated guanidines were synthesized in solid-phase from a primary amine source that was provided by the side chain of an Orn residue, by following a procedure that was previously described by our group. This methodology runs under mild conditions and employs aminium salts **13**, which are used as coupling reagents in solid-phase synthesis (Scheme 4).[18]

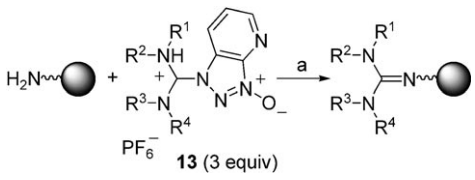

Scheme 4. Synthesis of tetraalkylated guanidine compounds. Reagents and conditions: a) DIEA (3 equiv), DMF, room temperature.

Solid-phase synthesis of ketones from the α-chloromethylketone of aspartic acid. The methodology that was followed was based on that previously described.[25] Semicarbazide resin **9** was treated with a solution of the α-chloromethylketone of aspartic acid **8** (3 equiv) in CH_2Cl_2, to afford the corresponding imine in quantitative yields.[28] The chloride displacement was then per-

formed with distinct nucleophiles, such as thiols, alcohols and secondary amines, in the presence of *N*,*N*-diisopropylethylamine (DIEA) as base. When thiols were used as nucleophiles, high yields of the desired thiomethyl ketones were obtained. In contrast, alcohols and secondary amines proved to be poor nucleophiles.

Solid-phase elongation. The Fmoc-*t*Bu strategy was followed for the synthesis of all the compounds described below. Once the Asp-based aldehyde or ketone was attached, the residues were coupled by using the Fmoc-aa-OH (5 equiv) with 1,3-diisopropylcarbodiimide (DIC, 5 equiv) and 1-hydroxybenzotriazole (HOBt, 5 equiv) in CH_2Cl_2, if not described otherwise. After optimization of the cleavage conditions, a mixture of TFA/H_2O (1:4) was found to be the most convenient. This acidic mixture hydrolyzed the imine bond, and also removed the *t*Bu-based protecting groups, but the Pbf protecting group of Arg was stable.

Compound characterization

13: 2.7 mg (39% yield, 93% purity); t_R: 6.7 min; ESI-MS: *m/z* calcd: 344.1, found: 344.3 $[M+H]^+$; *m/z* calcd: 362.3, found: 362.3 $[M+H_3O]^+$. **14**: 3.8 mg (53% yield, 95% purity); t_R: 7.1 min; ESI-MS: *m/z* calcd: 358.1, found: 358.3 $[M+H]^+$; *m/z* calcd: 376.14, found: 376.3 $[M+H_3O]^+$. **15**: 6.2 mg (49% yield, 95% purity); t_R: 9.2 min; ESI-MS: *m/z* calcd: 637.26, found: 637.4 $[M+H]^+$; *m/z* calcd: 655.28, found: 655.4 $[M+H_3O]^+$. **15a:** 6.6 mg (52% yield, 97% purity); t_R: 15.3 min (gradient 0→50%); ESI-MS: *m/z* calcd: 637.2, found: 637.6 $[M+H]^+$. **16**: 6.4 mg (54% yield, 94% purity); t_R: 8.5 min; ESI-MS: *m/z* calcd: 597.2, found: 597.4 $[M+H]^+$; *m/z* calcd: 615.2, found: 615.4 $[M+H_3O]^+$. **17**: 6.0 mg (56%, 97% purity); t_R: 7.3 min; ESI-MS: *m/z* calcd: 539.18, found: 539.3 $[M+H]^+$; *m/z* calcd: 557.20, found: 557.3 $[M+H_3O]^+$. **19**: 4.3 mg (50% yield, 92% purity); t_R: 6.6 min; ESI-MS: *m/z* calcd: 430.1, found: 430.3 $[M+H]^+$; *m/z* calcd: 448.1, found: 448.3 $[M+H_3O]^+$. **20**: 5.0 mg (50% yield, 97% purity); t_R: 9.3 min; ESI-MS: *m/z* calcd: 503.25, found: 503.5 $[M+H]^+$. **21**: 4.9 mg (44% yield, 98% purity); t_R: 9.2 min; ESI-MS: *m/z* calcd: 495.29, found: 495.5 $[M+H]^+$. **22**: 4.9 mg (48% yield, 98% purity); t_R: 8.6 min; EM-ESI-MS: *m/z* calcd: 493.2, found: 493.4 $[M+H]^+$. **23**: 5.2 mg (52%) yield, 98% purity); t_R: 10.1 min; ESI-MS: *m/z* calcd: 521.30, found: 521.4 $[M+H]^+$. **24**: 4.4 mg (43% yield, 93% purity); t_R: 6.0 min; ESI-MS: *m/z* calcd: 439.22, found: 439.6 $[M+H]^+$. **25**: 3 mg (85% yield, 92% purity); t_R: 4.6 min; ESI-MS: *m/z* calcd: 385.18, found: 385.5 $[M+H]^+$. **26**: 32 mg (67% yield, 98% purity); t_R: 9.1 min; ESI-MS: *m/z* calcd: 653.29, found: 653.5 $[M+H]^+$: *m/z* calcd: 671.31, found: 671.5 $[M+H_3O]^+$. **29**: 7.2 mg (49% yield, 98% purity); t_R: 12.3 min; ESI-MS: *m/z* calcd: 739.31, found: 739.3 $[M+H]^+$. **30**: 7.6 mg (50% yield, 94% purity). t_R: 12.2 min; ESI-MS: *m/z* calcd: 772.3, found: 772.3 $[M+H]^+$. **31**: 1.7 mg (12% yield, 91% purity); t_R: 11.6 min; ESI-MS: *m/z* calcd: 722.4, found: 722.3 $[M+H]^+$. **32**: 2.8 mg (19% yield, 90% purity); t_R: 10.9 min; ESI-MS: *m/z* calcd: 741.3, found: 741.3 $[M+H]^+$. **33**: t_R: 10.2 min; ESI-MS: *m/z* calcd: 725.3, found: 725.2 $[M+H]^+$. **34:** 1.8 mg (12% yield, 91% purity; t_R: 8.7 min; ESI-MS: *m/z* calcd: 736.4, found: 736.2 $[M+H]^+$. **35**: 1.9 mg (13% yield, 92% purity); t_R: 8.4 min; ESI-MS: *m/z* calcd: 734.3, found: 734.2 $[M+H]^+$.

Biological assays

Materials. Doxycycline hyclate, doxorubicin hydrochloride, tissue-culture grade dimethyl sulfoxide (DMSO), 3-(4,5-dimethylthiazol-2-yl)-2,5-diphenyl tetrazolium bromide (MTT), 0.4% trypan blue solution (cell culture grade), and dithiothreitol (DTT) were purchased from Sigma–Aldrich. 0.25% trypsin–EDTA, fetal calf serum (FCS), RPMI 1640 with L-glutamine, D-MEM with L-glutamine and L-glutamine were purchased from Gibco BRL Life Technologies (Paisley, UK). The fluorogenic and colorimetric caspase-3 substrates Ac-DEVD-afc and Ac-DVED-*p*Na were purchased from Biomol International LP (Exeter, UK) and Calbiochem (San Diego, CA, USA), respectively. Protein quantification was performed with a bicinchoninic acid kit from Pierce Biotechnology (New Jersey, USA). Active caspase-3 production involved folding from its large and small subunits; these were expressed separately in *E. coli*.[29] A colorimetric assay was used for the in vitro assays.[29]

Cell culture and culture conditions. The HEK 293 human embryonic kidney cell line was purchased from the German Collection of Microorganism and Cell Cultures (Braunschweig, Germany) and was grown in Dulbecco's modified Eagle's medium (DMEM) supplemented with 15% FCS and 2 mM L-glutamine. The U-937 human histiocytic lymphoma was obtained from the American Type Culture Collection (Rockville, MD, USA). The cells were grown in suspension in RPMI 1640 medium that was supplemented with 10% FCS, and 2 mM L-glutamine. The Saos-2 human osteosarcoma cell line was kindly provided by Karin Vousden (Cancer Research UK, Glasgow, UK) and cells were grown in DMEM that was supplemented with 15% FCS. Cells were maintained at 37 °C in an atmosphere of 5% CO_2 and 95% air and underwent passage twice weekly. The HEK 293 cell extract was performed and analyzed as described.[19,30] An MTT cell-viability assay was used to measure cell recovery and the putative toxicity of the compounds under evaluation in the distinct cell lines.[19] Briefly, cells were seeded in sterile 96-well microtiter plates at a density of 10^4 cells/well for Saos-2 and 4×10^3 cells per well for U937, and allowed to settle for 24 h. Doxycycline (2 μg mL^{-1} in PBS) for Saos-2 cells and doxorubicin in the case of U-937 at concentrations of 0.25 μg mL^{-1} in PBS were used. Compounds were added to cells 1 h before the cytotoxic agents. After 19 h of incubation, MTT (20 μL of a 5 mg mL^{-1} solution) was added to each well, and the cells were further incubated for 5 h. After removal of the medium, the precipitated formazan crystals were dissolved in optical grade DMSO (100 μL), and the plates were read at 570 nm with a Wallac 1420 workstation.

Molecular modeling

Starting structures for molecular dynamics studies of the various compounds synthesized were generated using the X-ray crystal structure of the caspase-3–Ac-DEVD-CHO complex (entry 1PAU of the Protein Data Bank) as scaffold.[31] The structures where generated by using the ChemDraw Ultra 8.0 software, and were later superposed manually onto the active center of caspase-3 by using the Insight II software. All calculations were carried out with the AMBER7 suite of programs.[32] The Parm94 force field[33] was used for natural amino acids except for the hydantoin ring, which was modeled using the gaff parameters.[32] Complexes were solvated with a cap of TIP3 waters with a radius of 25 Å in such a way that all the atoms that were involved in the receptor–ligand interaction region were solvated. Water molecules were subjected to a soft harmonic potential to restrain their movements. Nonbonded interactions were computed with a cutoff of 12 Å, and a distance-dependent dielectric constant of 1r was used for the electrostatic contribution. Energy minimizations were carried out in two steps of 1000 cycles of optimization. In the first minimization, all atoms were allowed to move, and in the second one the movement of caspase-3 residues with a distance greater than 15 Å away from the ligand were fixed. The optimized structures were used as a starting point to run molecular dynamics simulations. Molecular dynamics trajectories were computed at a constant temperature of

300 K by coupling the system to a thermal bath by using Berendsen's algorithm.[34] Initial structures were heated from 0 K to 300 K in 2 ps and, after 110 ps of molecular dynamics to equilibrate the systems, 100 ps of molecular dynamics were used to analyze receptor–ligand interactions.

Acknowledgements

This work was partially supported by CICYT (BIO2004-998, CTQ2006-06588/BQU, and CTQ2006-03794/BQU), Instituto de Salud Carlos III (CB06-01-0074), the Generalitat de Catalunya (2005SGR 00662), Centro de Investigación Príncipe Felipe, the Institute for Research in Biomedicine, and the Barcelona Science Park.

Keywords: apoptosis · combinatorial chemistry · cysteine proteases · molecular modeling · solid-phase synthesis

[1] J. F. Kerr, A. H. Wyllie, A. R. Currie, *Br. J. Cancer* **1972**, *26*, 239.
[2] M. O. Hengartner, *Nature* **2000**, *407*, 770.
[3] G. S. Salvesen, V. M. Dixit, *Cell* **1997**, *91*, 443.
[4] H. Y. Chang, X. Yang, *Microbiol. Mol. Biol. Rev.* **2000**, *64*, 821.
[5] S. W. Fesik, *Nat. Rev. Cancer* **2005**, *5*, 876.
[6] A. Nencioni, F. Grunebach, F. Patrone, A. Ballestrero, P. Brossart, *Crit. Rev. Immunol.* **2006**, *26*, 487.
[7] G. Takemura, H. Fujiwara, *J. Cell. Mol. Med.* **2006**, *10*, 56.
[8] M. P. Mattson, G. Kroemer, *Trends Mol. Med.* **2003**, *9*, 196.
[9] R. V. Talanian, K. D. Brady, V. L. Cryns, *J. Med. Chem.* **2000**, *43*, 3351.
[10] D. Chereau, L. Kodandapani, K. J. Tomaselli, A. P. Spada, J. C. Wu, *Biochemistry* **2003**, *42*, 4151.
[11] N. A. Thornberry, T. A. Rano, E. P. Peterson, D. M. Rasper, T. Timkey, M. Garcia-Calvo, V. M. Houtzager, P. A. Nordstrom, S. Roy, J. P. Vaillancourt, K. T. Chapman, D. W. Nicholson, *J. Biol. Chem.* **1997**, *272*, 17907.
[12] D. A. Allen, P. Pham, I. C. Choong, B. Fahr, M. T. Burdett, W. Lew, W. L. DeLano, E. M. Gordon, J. W. Lam, T. O'Brien, D. Lee, *Bioorg. Med. Chem. Lett.* **2003**, *13*, 3651.
[13] F. G. Gervais, D. Xu, G. S. Robertson, J. P. Vaillancourt, Y. Zhu, J. Huang, A. LeBlanc, D. Smith, M. Rigby, M. S. Shearman, E. E. Clarke, H. Zheng, L. H. van der Ploeg, S. C. Ruffolo, N. A. Thornberry, S. Xanthoudakis, R. J. Zamboni, S. Roy, D. W. Nicholson, *Cell* **1999**, *97*, 395.
[14] C. W. Scott, C. Sobotka-Briner, D. E. Wilkins, R. T. Jacobs, J. J. Folmer, W. J. Frazee, R. V. Bhat, S. V. Ghanekar, D. Aharony, *J. Pharmacol. Exp. Ther.* **2003**, *304*, 433.
[15] H. R. Stennicke, G. S. Salvesen, *J. Biol. Chem.* **1997**, *272*, 25719.
[16] T. O'Brien, D. Lee, *Mini-Rev. Med. Chem.* **2004**, *4*, 153.
[17] J. Vazquez, PhD Dissertation, University of Barcelona (Barcelona), **2005**.
[18] M. del Fresno, A. El-Faham, L. A. Carpino, M. Royo, F. Albericio, *Org. Lett.* **2000**, *2*, 3539.
[19] G. Malet, A. G. Martín, M. Orzáez, M. J. Vicent, I. Masip, G. Sanclimens, A. Ferrer-Montiel, I. Mingarro, A. Messeguer, H. O. Fearnhead, E. Pérez-Payá, *Cell Death Differ.* **2006**, *13*, 1523.
[20] H. O. Fearnhead, *Methods Cell Biol.* **2001**, *66*, 167.
[21] Y. Tsujimoto, *Genes Cells* **1998**, *3*, 697.
[22] D. R. Goode, A. K. Sharma, P. J. Hergenrother, *Org. Lett.* **2005**, *7*, 3529.
[23] L. A. Carpino, H. Shroff, S. A. Triolo, E. S. M. E. Mansour, H. Wenschuh, F. Albericio, *Tetrahedron Lett.* **1993**, *34*, 7829.
[24] J. Vazquez, F. Albericio, *Tetrahedron Lett.* **2002**, *43*, 7499.
[25] J. Vazquez, F. Albericio, *Tetrahedron Lett.* **2006**, *47*, 1657.
[26] J. Vazquez, M. Royo, F. Albericio, *Lett. Org. Chem.* **2004**, *1*, 224.
[27] M. Royo, W. van den Nest, M. del Fresno, A. Frieden, D. Yahalom, M. Rosemblatt, M. Chorev, F. Albericio, *Tetrahedron Lett.* **2001**, *42*, 7387.
[28] W. S. Hancock, J. E. Battersby, *Anal. Biochem.* **1976**, *71*, 260.
[29] M. Garcia-Calvo, E. P. Peterson, B. Leiting, R. Ruel, D. W. Nicholson, N. A. Thornberry, *J. Biol. Chem.* **1998**, *273*, 32608.
[30] H. O. Fearnhead, *Meth. Cell Biol.* **2001**, *66*, 167.
[31] J. Westbrook, Z. Feng, L. Chen, H. Yang, H. M. Berman, *Nucleic Acids Res.* **2003**, *31*, 489.
[32] D. A. Case, J. W. Pearlman, T. E. Caldwell, J. Wang, W. S. Ross, C. L. Simmerling, T. A. Darden, K. M. Merz, R. V. Stanton, A. L. Cheng, J. J. Vincent, M. Crowley, V. Tsui, H. Gohlke, R. J. Radmer, Y. Duan, J. Pitera, I. Massova, G. L. Seibel, U. C. Sligh, P. K. Weiner, P. A. Kollman, AMBER7, University of California, San Francisco (USA) **2002**.
[33] W. D. Cornell, P. Cieplak, C. I. Bayly, I. R. Gould, K. M. Merz, D. M. Ferguson, D. C. Spellmeyer, T. Fox, J. W. Caldwell, P. A. Kollman, *J. Am. Chem. Soc.* **1995**, *117*, 5179.
[34] H. Berendsen, J. Postman, W. Van Gunsteren, A. Dinola, J. Haak, *J. Chem. Phys.* **1984**, *81*, 3684.

Received: January 26, 2008
Revised: February 24, 2008
Published online on April 4, 2008

